SURE 静岡大学学術リポジトリ
Shizuoka University REpository

# Production and detection of reducing and oxidizing radicals in the catalytic decomposition of H⊠/O⊠ mixtures on heated tungsten surfaces



| メタデータ | 言語: en<br>出版者: American Institute of Physics<br>公開日: 2008-02-26<br>キーワード (Ja):<br>キーワード (En):<br>作成者: Umemoto, Hironobu, Moridera, Masashi<br>メールアドレス:<br>所属: |
|---|---|
| URL | http://hdl.handle.net/10297/606 |

# Production and detection of reducing and oxidizing radicals in the catalytic decomposition of $H_2/O_2$ mixtures on heated tungsten surfaces

Hironobu Umemoto[a)] and Masashi Moridera

*Faculty of Engineering, Shizuoka University, Johoku, Naka, Hamamatsu, Shizuoka 432-8561, Japan*

H atoms, O atoms, and OH radicals were identified in the catalytic decomposition of $H_2/O_2$ mixtures on heated polycrystalline tungsten surfaces. In order to suppress the oxidization of the tungsten catalyzer surfaces, the $H_2/O_2$ pressure ratio was kept more than 83, while the catalyzer temperature was kept below 2000 K. The absolute density of H atoms was determined by a vacuum-ultraviolet laser absorption technique, while one-photon and two-photon laser-induced fluorescence techniques were employed to extend the dynamic range. Since the O-atom density was much smaller, only a vacuum-ultraviolet laser-induced fluorescence technique could be used for the detection. The absolute density could be estimated by comparing the induced fluorescence intensity with that for H atoms. OH radicals could be identified by a laser-induced fluorescence technique in the ultraviolet region. The absolute density was determined by comparing the induced fluorescence intensity with

that of Rayleigh scattering caused by Ar. The H-atom density decreased with the increase in the $O_2$ partial pressure stepwisely. The O-atom density increased with the $O_2$ partial pressure monotonously, but the increase was rather slow at low $O_2$ pressures. The OH-radical density showed saturation against the $O_2$ partial pressure. These results can be explained by the change in the coverage conditions of the catalyzer surfaces.

---

[a)]Electronic mail: thumemo(at)ipc.shizuoka.ac.jp

## I. INTRODUCTION

In catalytic chemical vapor deposition (Cat-CVD in short, often called Hot-Wire CVD) processes, the material gases are decomposed to radical species on resistively heated metal surfaces.[1,2] One of the weak points in this technique compared with plasma-enhanced CVD is that it is difficult to use oxidizing species such as $O_2$ as a material gas.[3] This is because tungsten, one of the most widely used catalyzer materials, is easily oxidized. It should also be remembered that the vapor pressure of tungsten oxide is higher than that of tungsten metal and this can be a cause of metal contamination. Recently, we have shown that the oxidization of W catalyzers can be diminished by the addition of an excess amount of $H_2$ or $NH_3$.[3] $O_2$, NO, and $N_2O$ were used as the oxidizing materials, and it was shown that the decomposition efficiency of $O_2$ is the highest. The introduction of oxidizing materials in catalytic CVD processes is currently desired to prepare films containing oxygen such as $Al_2O_3$, $SiO_2$, and $SiO_xN_y$.[3] $SiO_xN_y$ films can be used as a buffer layer to reduce the stress in $SiN_x$ films and to prevent the formation of micro slits in passivation films.[4] However, the mechanism of catalytic decomposition of oxidizing species has not been studied. Information on the decomposition mechanism is essential to choose the best conditions for deposition.

In the present work, H atoms, O atoms, and OH radicals produced by the catalytic decomposition on a heated tungsten filament in $H_2/O_2$ systems were detected by laser

spectroscopic techniques under various conditions. In addition, the consumption efficiencies of $O_2$ were measured by using a quadrupole mass spectrometric technique.

## II. EXPERIMENT

The experimental apparatus was similar to that described elsewhere, except for the reaction chamber.[5-8] A cylindrical reaction chamber with six ports made of stainless steel was used. The internal diameter was 10 cm. This chamber was evacuated with a turbo molecular pump (Osaka Vacuum, TG220FCAB). The inner walls of the chamber were coated with $SiO_2$ in order to reduce the removal rates of radical species. The procedure of $SiO_2$ coating was the same as that described previously.[8] The catalyzer was a coiled tungsten wire (Nilaco, 30 cm in length and 0.38 mm in diameter, 99.95%) and was resistively heated by using a DC power supply (Takasago, EX-1125H2). The distance between the catalyzer and the detection zone by laser beams was 9 cm. The catalyzer temperature was estimated from the resistivity. The flow rate of $H_2$ was fixed at 100 sccm (1 sccm = $6.9 \times 10^{-7}$ mol $s^{-1}$) by using a mass flow controller (STEC, SEC-400MK3). The $H_2$ pressure, measured with a capacitance manometer, was 17 Pa otherwise stated. The flow rate of $O_2$ was changed between 0.00 and 1.20 sccm by using another mass flow controller (STEC, SEC-7320M).

Four laser spectroscopic techniques were employed to measure the H-atom densities.

The first one was the vacuum-ultraviolet (vuv) laser absorption technique at 121.6 nm.[5-8] By this technique, it is possible to determine the absolute densities. The problem is that the dynamic range is rather narrow and restricted to the order of $10^{11}$ $cm^{-3}$. The second technique was vacuum-ultraviolet laser-induced fluorescence (vuv LIF).[9,10] This technique is more sensitive than the absorption technique, but cannot be employed when the H-atom density is high. When the H-atom density is higher than $5\times10^{10}$ $cm^{-3}$, the system is optically too thick and the vuv laser beam cannot reach the center of the chamber. The measurement by this technique was necessary to estimate the O-atom density, which could only be measured with this vuv LIF technique. The third one was the two-photon laser-induced fluorescence technique at 243.2 nm to excite to H(2s $^2$S).[11,12] H(2s $^2$S) can easily be collisionally relaxed to the near-by 2p $^2P_J$ states, which fluoresce Lyman-α at 121.6 nm. This technique is also sensitive, but cannot be employed when the H-atom density is high, either. This is because Lyman-α can easily be trapped and the upper H(2p $^2$P) states can easily be quenched by $H_2$ and the quantum efficiency of the fluorescence should depend on the H-atom density. The rate constant for the quenching of H(2p $^2$P) by $H_2$ has been reported to be as large as $2.5 \times 10^{-9}$ $cm^3s^{-1}$.[13] The fourth technique was two-photon laser-induced fluorescence at 205.1 nm to excite to H(3s $^2$S, 3d $^2$D) and to observe Balmer-α at 656.3 nm.[5] This technique is less sensitive, but can be used in the presence of an excess amount of H atoms since radiation

trapping is not expected in this visible transition. In the present work, the vuv absorption technique was employed to determine the absolute densities. The relative values obtained by LIF techniques were scaled to the absolute ones by comparing the signal intensities where absolute values are available from the absorption technique.

The procedure of the vuv laser absorption technique was similar to that reported previously.[5-8] The absorption path length was 15 cm. A dye laser (Quanta-Ray, PDL-3) pumped with a Nd:YAG (YAG denotes yttrium aluminum garnet) laser (Quanta-Ray, GCR-170 or PRO-190) was used as a light source. The output of the dye laser around 729.6 nm was doubled in frequency by a $KH_2PO_4$ (KDP) crystal and then tripled by a mixture of Kr and Ar. The resulting vuv light was collimated with a 100-mm focal-length $MgF_2$ lens (Oken), and the intensity after passing through the chamber was measured by monitoring the $NO^+$ ion current.

The procedure of the vuv LIF technique was also similar to that described elsewhere.[9,10] The laser system was the same as that used for the vuv laser absorption measurements. The induced fluorescence was detected with a solar-blind photomultiplier tube (Hamamatsu Photonics, R6835) through an $MgF_2$ collimating lens and an interference filter (Acton Research, 122-N).

The procedures of the two-photon LIF techniques, both at 243.2 nm and at 205.1 nm, were also similar to those employed in previous studies.[5,11,12] The laser pulse at 243.2 nm was

produced by doubling the output of a dye laser by a β-$BaB_2O_4$ (BBO) crystal, while that at 205.1 nm was produced by tripling the output by using two BBO crystals and a polarizer. The detection system to observe Lyman-α was the same as that used for vuv LIF. The Balmer-α fluorescence was detected with a photomultiplier tube (Hamamatsu Photonics, R212UH) through an interference filter (Nihon Shinku Kogaku).

In the detection of O atoms, only the vuv LIF technique at 130.2 nm could be employed. Other techniques, such as vuv laser absorption and two-photon LIF at 225.7 nm,[14] were tried but the sensitivities were too low. The laser pulse at 130.2 nm was produced by a four-wave mixing technique.[15] Two dye lasers (both Quanta Ray, PDL-3) were pumped with a Nd:YAG laser (Quanta-Ray, PRO-190) simultaneously. The output of one of the dye lasers was tripled and the wavelength was fixed at 216.7 nm, which is resonant to the $4p^5 5p\ ^2[3/2]_2$ – $4p^6\ ^1S_0$ transition of Kr. The output of another dye laser was scanned around 644.6 nm. The pulse energies of the lasers were 0.6 and 6 mJ, respectively. The two laser beams were combined and made collinear at a beam combiner and were focused into a vessel filled with 2.7 kPa of Kr by using a 100-mm focal-length achromatic lens to produce 130.2-nm radiation.

OH radicals were detected by employing an LIF technique in the ultraviolet region, which corresponds to the (0,0) band of the $A\ ^2\Sigma^+ - X\ ^2\Pi$ transition.[12,16] The output of a dye laser was doubled in frequency by a KDP crystal installed in an autotracker (Inrad, Autotracker

III). The pulse energy of the probe laser was typically 10 μJ, which was weak enough not to saturate the transitions.

The absolute density of OH radicals was evaluated by comparing the LIF intensity under saturated conditions with the intensity of Rayleigh scattering caused by Ar. The procedure was similar to that employed for the absolute density measurements of Si, SiH, NH, and $NH_2$.[6,17] During the laser pulse, since the duration time of the laser is just 5 ns, collisional quenching or rotational state mixing can be ignored. On the other hand, the radiative lifetime of the upper $A\ ^2\Sigma^+$ state is much longer and the quenching process by $H_2$ cannot be ignored.[18,19] Then, the decay profiles of the induced fluorescence were recorded with a digital oscilloscope (LeCroy, 6051A) to evaluate the fluorescence yields. OH($A\ ^2\Sigma^+$, $v'$=0) may fluoresce not only *via* the (0,0) band around 308 nm but also *via* the (0,1) band around 346 nm. Since the wavelength of Rayleigh scattering is exactly the same as that of the excitation laser, this can be a cause of an error in the determination of the absolute densities. However, the change in the sensitivity of the detection system is rather small and this was not taken into account in the present evaluation of the absolute densities.

Mass spectrometric analysis was also carried out to measure the decomposition efficiency of $O_2$. The experimental procedure was similar to that described elsewhere.[3,5] A quadrupole mass-spectrometer (Anelva, M-QA200TS) was attached to the chamber through a

sampling hole (0.1 mm in diameter). The flight tube was differentially pumped down to $5 \times 10^{-4}$ Pa with a turbo molecular pump (Osaka Vacuum, TG350FCWB).

$H_2$ (Japan Air Gases, 99.999%), $O_2$ (Takachiho, 99.99%), Kr (Nihon Sanso, 99.995%), Ar (Japan Air Gases, 99.999%), and NO (Nihon Sanso, 99%) were used from cylinders without further purification.

## III. RESULTS

Figure 1 shows the vacuum-ultraviolet laser-absorption spectra of H atoms. The $H_2$ flow rate was 100 sccm and the catalyzer temperature was 1700 K. The spectral profiles are consistent with the translational temperature of 450 K. The $O_2$ flow rate dependence of the H-atom density measured with the vuv laser-absorption technique at 1700 K and those with the two-photon LIF technique at 243.2 nm at 1700 and 1800 K are plotted in Fig. 2. Consistent results were obtained at 1700 K when two different techniques were used. In both cases, the H-atom densities depend little on the $O_2$ flow rate when the flow rate is less than 0.3 sccm, while they decrease rapidly when the flow rate is over 0.3 sccm. Figure 3 illustrates the similar results at 1800, 1900, and 2000 K obtained by the two-photon LIF technique at 205.1 nm. At these high catalyzer temperatures, the decrease is more gradual than those at lower temperatures.

Figure 4 shows the vuv LIF spectra of O atoms in $H_2/O_2$ systems at various $O_2$ flow rates. The catalyzer temperature was 2000 K. The integrated intensity is plotted against the $O_2$ flow rate in Fig. 5. The absolute density of O atoms was estimated by a procedure given below. The dashed line represents the least-squares fit excluding the origin. The intercept is negative. In other words, the increase is slow when the $O_2$ flow rate is low. When the catalyzer temperature was 1900 K, the O-atom density was smaller by a factor of 4.

The absolute density of O atoms was estimated by comparing the vuv LIF signal intensities of H and O atoms. Figure 6 shows a comparison of the LIF spectra of H and O atoms. The H-atom spectrum was recorded in the presence of 100 sccm of $H_2$ flow without $O_2$, while that for O atoms was recorded in the presence of 100 sccm of $H_2$ flow and 1.20 sccm of $O_2$ flow. The catalyzer temperatures were 1600 and 2000 K, respectively. The total pressure was 17 Pa in both cases. The voltage applied to the photomultiplier tube was 1300 V for H atoms and 1700 V for O atoms. The density of H atoms evaluated from the vuv laser absorption measurement under the above conditions is $1.1 \times 10^{11}$ $cm^{-3}$. The integrated LIF signal intensity for H atoms was 3.7 times larger than that for O atoms when exactly the same detection system was used. Here, several corrections are necessary to evaluate the absolute density of O atoms. First, the transmittance of Lyman-α laser when the path length was 15 cm was 71% in the presence of $1.1 \times 10^{11}$ $cm^{-3}$ of H atoms. The LIF path length was similar

and the LIF signal for H atoms may have been reduced by this factor by optical absorption. The O-atom signal may not have been affected by such an absorption effect. The laser pulse at 130.2 nm to detect O atoms, measured by $NO^+$ ion current, was twice more intense compared with that at 121.6 nm to detect H atoms. The linearity between the laser intensity and the LIF signal was, of course, confirmed. In the vacuum-ultraviolet laser intensity measurements, it was assumed that the absorption coefficients of NO at 121.6 nm and 130.2 nm are the same. This assumption is supported by the measurement by Marmo.[20] It was also assumed that the efficiencies of NO ionization are the same. The photomultiplier signal increases by a factor of 14 when the applied voltage is increased from 1300 to 1700 V. The effective absorption coefficient for H atoms is 4.9 times larger than that for O atoms. This factor was evaluated by numerical calculations by assuming Doppler widths at 450 K. In the present LIF measurement, only the $^3P_2$ state of O atoms was detected. The ratio of the total population of O atoms to that of $O(^3P_2)$ is 1.5 at 450 K. It should be noted that this ratio depends only weakly on the electronic temperature assumed, since the intramultiplet splittings are small. The transmittance of the interference filter at 121.6 nm is 3.3 times larger than that at 130.2 nm. The wavelength dependence of the sensitivity of the photomultiplier tube is minor according to manufacturer's data. By taking into account these correction factors, the absolute density of O atoms under the conditions in Fig. 6(b) is estimated to be $1.8 \times 10^{10}$ $cm^{-3}$.

Since there are many correction factors, uncertainty by a factor of two may not be avoidable.

Figure 7 (a) shows the LIF spectrum of OH(X $^2\Pi$, $v''$=0). The catalyzer temperature was 1900 K. The flow rates of $H_2$ and $O_2$ were 100 and 0.40 sccm, respectively. Variation in laser pulse energies was corrected in this figure. The spectral lines were assigned according to the data reported by Dieke and Crosswhite.[21] Figure 7 (b) illustrates a simulated spectrum by assuming the rotational temperature of 350 K. This temperature may not represent that just after the formation since OH radicals may collide with $H_2$ molecules more than 100 times before being detected. In this simulation, the transition probabilities calculated by Dimpfl and Kinsey were employed.[22] The rotational level dependence of the rate constants for the quenching of OH(A $^2\Sigma^+$)[18,19] was not taken into account, since the determination of the rotational state distribution is not the main purpose of the present study. It was impossible to observe any LIF signals belonging to the (1,1) band around 314 nm. Taking into account the difference in Franck-Condon factors,[23] the yield of OH($v''$=1) is estimated to be less than 5% of that of OH($v''$=0).

Figure 8 shows that the OH-radical density saturates against the $O_2$ partial pressure. In this measurement, the $H_2$ flow rate was 100 sccm and the total pressure was 17 Pa. The catalyzer temperature was 2000 K. The absolute density of OH was evaluated by comparing the time integrated LIF intensity for the $P_1(N''=2, J''=5/2)$ transition at 308.6 nm, $I_{LIF}$, with the

intensity of Rayleigh scattering caused by Ar, $I_R$.[6,17] Here, $J''$ and $N''$ represent the total angular momentum quantum number exclusive of nuclear spin and that exclusive of nuclear and electron spin, respectively. This transition was chosen because that is satellite free. The ratio of $I_{LIF}$ to $I_R$ was 0.40 when the $O_2$ flow rate and the catalyzer temperature were 0.40 sccm and 2000 K, respectively. This ratio should be given by:

$$\frac{I_{LIF}}{I_R} = \frac{S_L}{N_0 \sigma E_L} \frac{h\nu}{4\pi} \varphi N^*.$$

Here, $N_0$ is the Ar density, $1.6 \times 10^{18}$ cm$^{-3}$, $S_L$ is the cross section of the laser beam, 0.20 cm$^2$, $\sigma$ is the differential cross section for Rayleigh scattering, $5.5 \times 10^{-27}$ cm$^2$, $E_L$ is the laser pulse energy in the Rayleigh scattering measurements, 0.33 mJ, $h\nu$ is the photon energy, $\varphi$ is the quantum yield of the fluorescence, and $N^*$ is the number density of excited OH radicals. In LIF measurements, the pulse energy was increased up to 2.0 mJ to saturate the transition. Under saturated conditions, the ratio of the population of the upper state, OH(A $^2\Sigma^+$, $v'$=0, $N'$=1, $J'$=3/2), to that of the lower state, OH(X $^2\Pi$, $v''$=0, $N''$=2, $J''$=5/2), before excitation is 1/3 when the excitation laser is linearly polarized.[24] The decay rate of the induced fluorescence was $2.16 \times 10^6$ s$^{-1}$, while the reported radiative decay rate of OH(A $^2\Sigma^+$, $v'$=0, $N'$=1) is $1.44 \times 10^6$ s$^{-1}$.[25] Then, the quantum yield for the fluorescence, $\varphi$, is calculated to be 0.67. It should be noted that the decay rate of OH(A $^2\Sigma^+$, $v'$=0, $N'$=1) measured in the present work is consistent with the rate constant for the quenching by $H_2$ reported by Copeland *et al.*,

$2.13 \times 10^{-10}$ $cm^3s^{-1}$.[18,19] When a Boltzmann distribution at 350 K is assumed, the ratio of the population of the lower level of the $P_1(N''=2, J''=5/2)$ transition to the total one is 0.082. Taking into account all these factors, the total population of OH is calculated to be $6.2 \times 10^9$ $cm^{-3}$. There is no large difference if different rotational temperatures were assumed. For example, if we assume a Boltzmann distribution at 450 K, the total density is calculated to be 20% smaller. The population when the catalyzer temperature was 1900 K was 1/3 of that at 2000 K.

The $H_2$ pressure dependences of the radical densities were also measured. The $O_2$ partial pressure and the $H_2$ flow rate were kept constant at 0.17 Pa and 100 sccm, respectively. The catalyzer temperature was 2000 K. In these measurements, since the diffusion coefficients of radicals, and consequently the removal rates, may change, quantitative analyses are difficult, but qualitative discussion may still be possible. The H-atom and OH-radical densities increased by factors of 3 and 2, respectively, when the $H_2$ pressure was increased from 17 to 34 Pa. On the other hand, the O-atom density decreased by a factor of 3.

According to quadrupole mass-spectrometric measurements, the decomposition efficiency of $O_2$ was determined to be 16% when the catalyzer temperature was 2000 K and the flow rates of $H_2$ and $O_2$ were 100 and 1.00 sccm, respectively. This is a little smaller than that reported previously.[3] The main cause of the difference may be ascribed to the difference in

the catalyzer length. Slight increase in the mass spectrometric signal of $H_2O^+$ was observed when the catalyzer was heated, but it is not clear if $H_2O$ molecules are produced on the catalyzer surfaces directly or produced in secondary processes.

## IV. DISCUSSION

The present results can be explained by a catalytic decomposition model presented schematically in Fig. 9. In the present study, the steady-state densities of radical species in the gas phase were measured. In general, the steady-state densities depend not only on the production rates, but also on the removal rates, and the densities may not represent the production rates only. However, the removal rates may not change greatly by the addition of a small amount of $O_2$, since no deposition takes place and there should be no large changes in the wall conditions. It should also be remembered that the gas-phase rate constants for $O+H_2$, $OH+H_2$, and $H+O_2$ reactions are all extremely small below 500 K, both for bimolecular and termolecular processes.[26-29] The temperature near the catalyzer may be high, but the temperature may decrease rapidly with the distance. The rotational temperatures of SiH, NH, and CN radicals produced by the catalytic decomposition of $SiH_4$, $NH_3$, and HCN, respectively, have been measured to be below 500 K.[6,17,30] These low temperatures suggest the presence of efficient collisional relaxation processes in the gas phase. The rotational temperature of $H_2$

has been measured to be 670 K when the catalyzer was heated up to 2700 K in the presence of 67 Pa of $H_2$, but it should be noted that the rotational temperature decreases not only with the decrease in catalyzer temperature but also with that in $H_2$ pressure.[31] The vibrational excitation is also minor. The different behaviors of O-atom and OH-radical densities on the $O_2$ flow rate strongly suggest that OH radicals are not produced in gas-phase reactions between O and $H_2$. The $O_2$ flow rate dependences of the radical densities may represent the changes in the production rates on catalyzer surfaces.

When the $O_2$ partial pressure is low, the active sites occupied by O atoms must be sparse. H atoms adsorbed on the active sites can migrate on the surfaces and capture the O atoms to produce OH radicals. The surface density of H atoms may be higher than that of O atoms, but the surface fractional coverage by H atoms must be low when the catalyzer temperature is as high as 2000 K.[32] Under such conditions, only OH radicals are ejected besides H atoms, and possibly $H_2O$ molecules. The ejection of O atoms must be minor. If the residence time of O atoms on the catalyzer surfaces in the presence of an excess amount of adsorbed H atoms is short, the effect of poisoning must be minor and the number of H atoms ejected may depend little on the partial pressure of $O_2$. On the other hand, when the $O_2$ partial pressure is high, O atoms should be the main adsorbed species. Under such conditions, O atoms can be ejected. In the production of OH radicals, the increase in the adsorbed O-atom

density and the decrease in the H-atom density must be compensated. If some O atoms reside on the catalyzer surfaces under such conditions, *i.e.* in the absence of many adsorbed H atoms, the production of H atoms must be suppressed.

The $H_2$ pressure dependence of the radical densities is also consistent with the above model. The ejection rate of OH radicals may increase with the increase in the adsorbed H-atom density on the catalyzers, while that of O atoms may decrease. The increase in the OH-radical density as well as that in H atoms is consistent with the model that the surface fractional coverage by H atoms is low.[32] The residence time of H atoms on the catalyzer surfaces must be short.

Under the present experimental conditions, when the $O_2$ partial pressure is low or when the $H_2$ pressure is high, the OH density is higher than that of O atoms, while the O-atom density is higher when the $O_2$ pressure is high or the $H_2$ pressure is low. In any case, the densities of these oxidizing species are comparable and it may be concluded that both contribute to the oxidation.

## V. CONCLUSIONS

Reducing and oxidizing radicals in the catalytic decomposition of $H_2/O_2$ mixtures on heated tungsten filaments were identified. The H-atom density in the gas phase decreased

stepwisely with the increase in the $O_2$ partial pressure. The O-atom density increased with the $O_2$ partial pressure, but the increase rate was small at low $O_2$ pressures. The OH-radical density showed saturation against the $O_2$ partial pressure. Such $O_2$ partial pressure dependences of the radical densities can be explained by the change in the coverage conditions of the catalyzer surfaces. When the $O_2$ partial pressure is low, the main adsorbed species are H atoms and the active sites occupied by O atoms are sparse. Under such conditions, only OH radicals are ejected besides H atoms, and possibly $H_2O$ molecules. On the other hand, when the $O_2$ partial pressure is high, O atoms should be the main adsorbed species and O atoms can be ejected. OH radicals may also be ejected but the ejection rate is limited by the number of H atoms adsorbed.

**ACKNOWLEDGMENT**

This work was partially funded by the Grant-in-Aid for Science Research (No. 19550015) from the Japan Society for the Promotion of Science.

## References


[1] H. Matsumura, Jpn. J. Appl. Phys., Part 1 **37**, 3175 (1998).

[2] H. Matsumura, A. Masuda, and H. Umemoto, Thin Solid Films **501**, 58 (2006).

[3] H. Umemoto, S. G. Ansari, T. Morimoto, S. Setoguchi, H. Uemura, and H. Matsumura, Thin Solid Films in press.

[4] Y. Ogawa, K. Ohdaira, T. Oyaidu, and H. Matsumura, Thin Solid Films in press.

[5] H. Umemoto, K. Ohara, D. Morita, Y. Nozaki, A. Masuda, and H. Matsumura, J. Appl. Phys. **91**, 1650 (2002).

[6] H. Umemoto, K. Ohara, D. Morita, T. Morimoto, M. Yamawaki, A. Masuda, and H. Matsumura, Jpn. J. Appl. Phys., Part 1 **42**, 5315 (2003).

[7] T. Morimoto, H. Umemoto, K. Yoneyama, A. Masuda, H. Matsumura, K. Ishibashi, H. Tawarayama, and H. Kawazoe, Jpn. J. Appl. Phys., Part 1 **44**, 732 (2005).

[8] S. G. Ansari, H. Umemoto, T. Morimoto, K. Yoneyama, A. Masuda, H. Matsumura, M. Ikemoto, and K. Ishibashi, J. Vac. Sci. Technol. A **23**, 1728 (2005).

[9] H. Umemoto, J. Chem. Phys. **125**, 034306 (2006).

[10] H. Umemoto, J. Chem. Phys. **127**, 014304 (2007).

[11] H. Umemoto, T. Nakae, H. Hashimoto, K. Kongo, and M. Kawasaki, J. Chem. Phys. **109**, 5844 (1998).

[12] H. Umemoto, T. Asai, H. Hashimoto, and T. Nakae, J. Phys. Chem. A **103**, 700 (1999).

[13] G. Van Volkenburgh, T. Carrington, and R. A. Young, J. Chem. Phys. **59**, 6035 (1973).

[14] H. Umemoto, K. Tanaka, S. Oguro, R. Ozeki, and M. Ueda, Chem. Phys. Lett. **345**, 44 (2001).

[15] G. Hilber, A. Lago, and R. Wallenstein, J. Opt. Soc. Am. B **4**, 1753 (1987).

[16] K. Kuwahara, H. Ikeda, H. Umemoto, T. Sato, K. Takano, S. Tsunashima, F. Misaizu, and K. Fuke, J. Chem. Phys. **99**, 2715 (1993).

[17] Y. Nozaki, K. Kongo, T. Miyazaki, M. Kitazoe, K. Horii, H. Umemoto, A. Masuda, and H. Matsumura, J. Appl. Phys. **88**, 5437 (2000).

[18] R. A. Copeland and D. R. Crosley, Chem. Phys. Lett. **107**, 295 (1984).

[19] R. A. Copeland, M. J. Dyer, and D. R. Crosley, J. Chem. Phys. **82**, 4022 (1985).

[20] F. F. Marmo, J. Opt. Soc. Am. **43**, 1186 (1953).

[21] G. H. Dieke and H. M. Crosswhite, J. Quant. Spectrosc. Radiat. Trans. **2**, 97 (1962).

[22] W. L. Dimpfl and J. L. Kinsey, J. Quant. Spectrosc. Radiat. Trans. **21**, 233 (1979).

[23] R. W. Nicholls, Proc. Phys. Soc. **69A**, 741 (1956).

[24] A. Hirabayashi, Y. Nambu, and T. Fujimoto, Jpn. J. Appl. Phys., Part 1 **25**, 1563 (1986).

[25] K. R. German, J. Chem. Phys. **63**, 5252 (1975).

[26] D. L. Baulch, C. J. Cobos, R. A. Cox, C. Esser, P. Frank, Th. Just, J. A. Kerr, M. J.

Pilling, J. Troe, R. W. Walker, and J. Warnatz, J. Phys. Chem. Ref. Data **21**, 411 (1992).

[27] D. L. Baulch, C. J. Cobos, R. A. Cox, P. Frank, G. Hayman, Th. Just, J. A. Kerr, T. Murrells, M. J. Pilling, J. Troe, R. W. Walker, and J. Warnatz, J. Phys. Chem. Ref. Data **23**, 847 (1994).

[28] R. Atkinson, D. L. Baulch, R. A. Cox, J. N. Crowley, R. F. Hampson, R. G. Hynes, M. E. Jenkin, M. J. Rossi, and J. Troe, Atmos. Chem. Phys. **4**, 1461 (2004).

[29] J. A. Miller, M. J. Pilling, and J. Troe, Proc. Combust. Inst. **30**, 43 (2005).

[30] H. Umemoto, T. Morimoto, M. Yamawaki, Y. Masuda, A. Masuda, and H. Matsumura, J. Non-Cryst. Solids **338-340**, 65 (2004).

[31] H. Umemoto, S.G. Ansari, and H. Matsumura, J. Appl. Phys. **99**, 043510 (2006).

[32] W. Zheng and A. Gallagher, Surf. Sci. **600**, 2207 (2006).

**Figure Captions**

FIG. 1. Vacuum-ultraviolet laser-absorption spectra of H atoms. The $H_2$ flow rate was 100 sccm and the catalyzer temperature was 1700 K. The $O_2$ flow rate was 0.40 sccm, 0.35 sccm and 0.00 sccm from top to bottom. The total pressure was 17 Pa.

FIG. 2. H-atom densities as a function of $O_2$ flow rate measured by a vacuum-ultraviolet laser absorption technique (□) or a two-photon laser induced fluorescence technique at 243.2 nm *via* the 2s $^2$S state (● and ▲). The $H_2$ flow rate was 100 sccm and the total pressure was 17 Pa. The catalyzer temperatures were 1800 K (●) and 1700 K (□ and ▲). The absolute values were evaluated from absorption measurements.

FIG. 3. H-atom densities as a function of $O_2$ flow rate measured by a two-photon laser induced fluorescence technique at 205.1 nm *via* the 3s $^2$S or 3d $^2$D states. The $H_2$ flow rate was 100 sccm and the total pressure was 17 Pa. The catalyzer temperatures were 2000 K (△), 1900 K (○), and 1800 K (●). The absolute values were evaluated from absorption measurements.

FIG. 4. Vacuum-ultraviolet laser-induced fluorescence spectra of O atoms in $H_2/O_2$ systems. The $H_2$ flow rate was 100 sccm and the catalyzer temperature was 2000 K. The $O_2$ flow rate

was 1.20, 1.00, 0.80, 0.60, 0.40, and 0.20 sccm from top to bottom. The total pressure was 17 Pa.

FIG. 5. O-atom densities as a function of $O_2$ flow rate. The $H_2$ flow rate was 100 sccm and the total pressure was 17 Pa. The catalyzer temperature was 2000 K. The dashed line represents the least-squares fit excluding the origin.

FIG. 6. Vacuum-ultraviolet laser-induced fluorescence spectra of H and O atoms. The experimental conditions were: (a) The $H_2$ flow rate was 100 sccm without $O_2$ flow. The catalyzer temperature was 1600 K and the applied voltage to the photomultiplier tube was 1300 V. (b) The flow rates of $H_2$ and $O_2$ were 100 and 1.20 sccm, respectively. The catalyzer temperature was 2000 K and the applied voltage to the photomultiplier tube was 1700 V. The total pressure was 17 Pa in both systems.

FIG. 7. (a) Laser-induced fluorescence spectrum of OH radicals measured in the presence of 100 sccm of $H_2$ and 0.40 sccm of $O_2$ flow. The total pressure was 17 Pa. The catalyzer temperature was 1900 K. The assignments are shown for the $P_1$, $Q_1$, $Q_2$, and $R_2$ branches of the (0,0) band. The numbers are the total angular momentum quantum numbers exclusive of

nuclear and electron spin. (b) Simulated spectrum of OH. The rotational temperature was assumed to be 350 K.

FIG. 8. OH-radical densities as a function of $O_2$ flow rate. The $H_2$ flow rate was 100 sccm and the total pressure was 17 Pa. The catalyzer temperature was 2000 K.

FIG. 9. Schematic diagram to explain the $O_2$ partial pressure dependence of the H-atom, O-atom, and OH-radical densities.

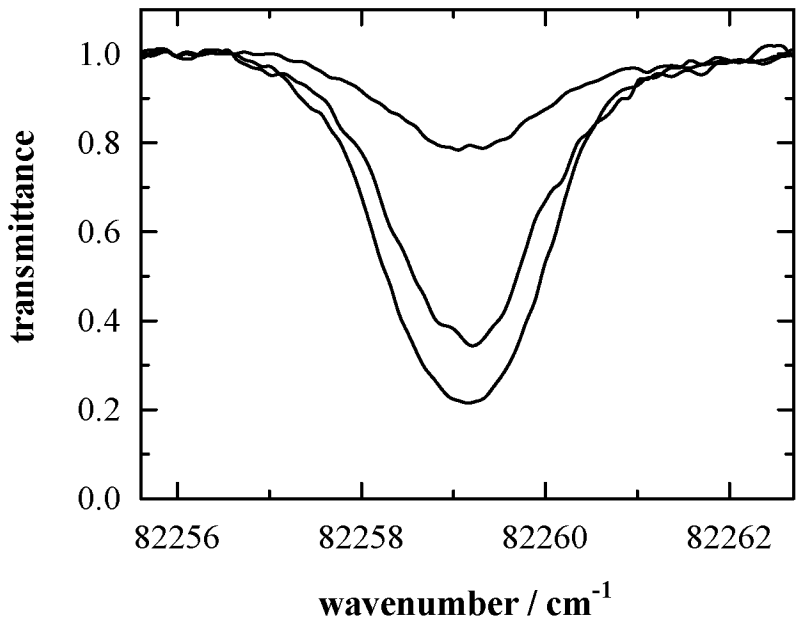


Fig. 1 H. Umemoto and M. Moridera

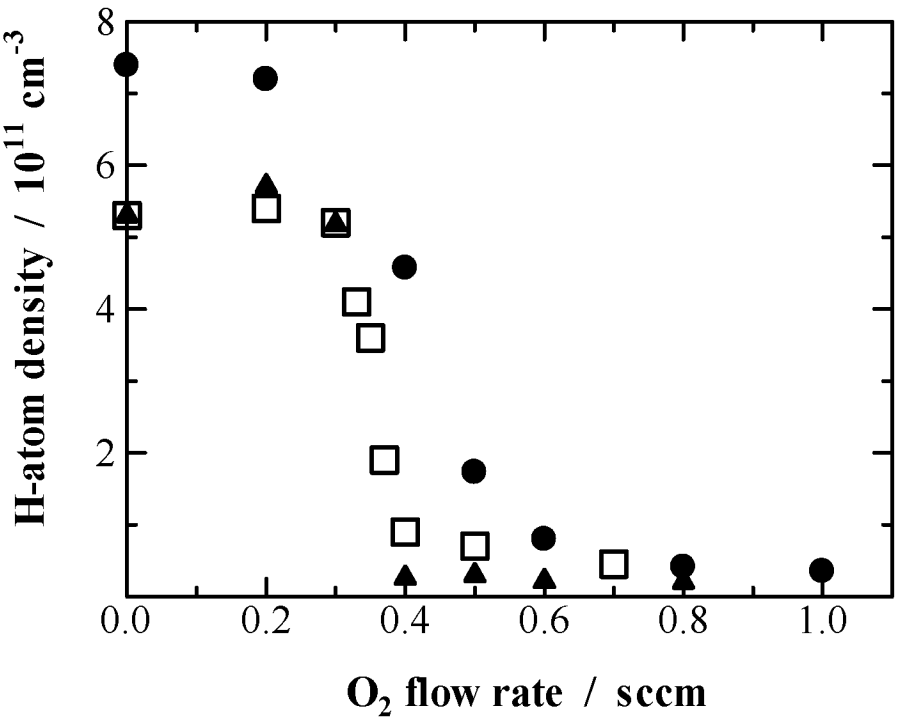


Fig. 2. H. Umemoto and M. Moridera

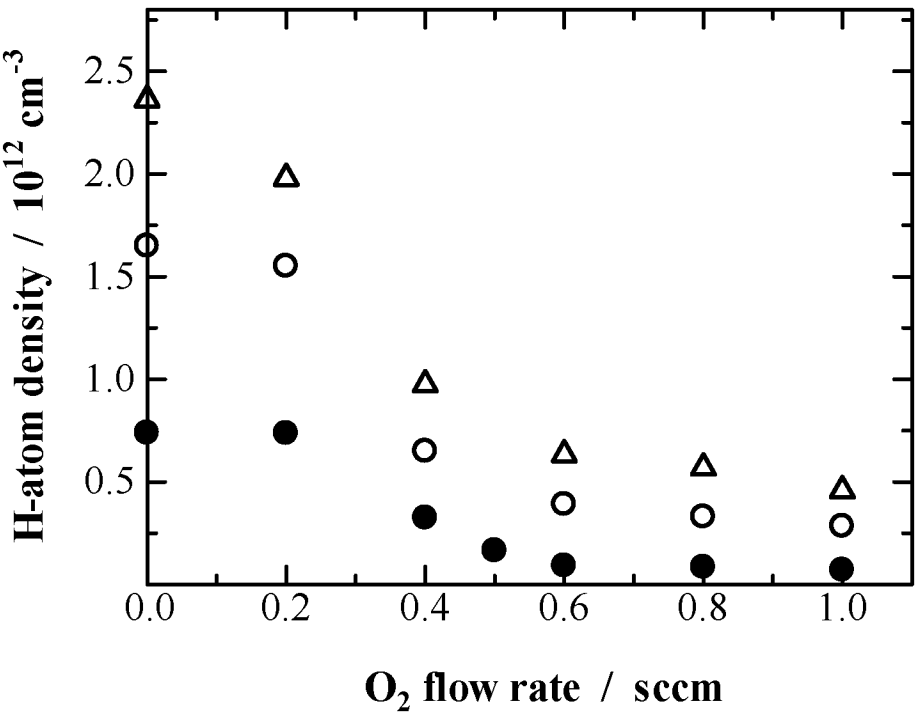


Fig. 3. H. Umemoto and M. Moridera

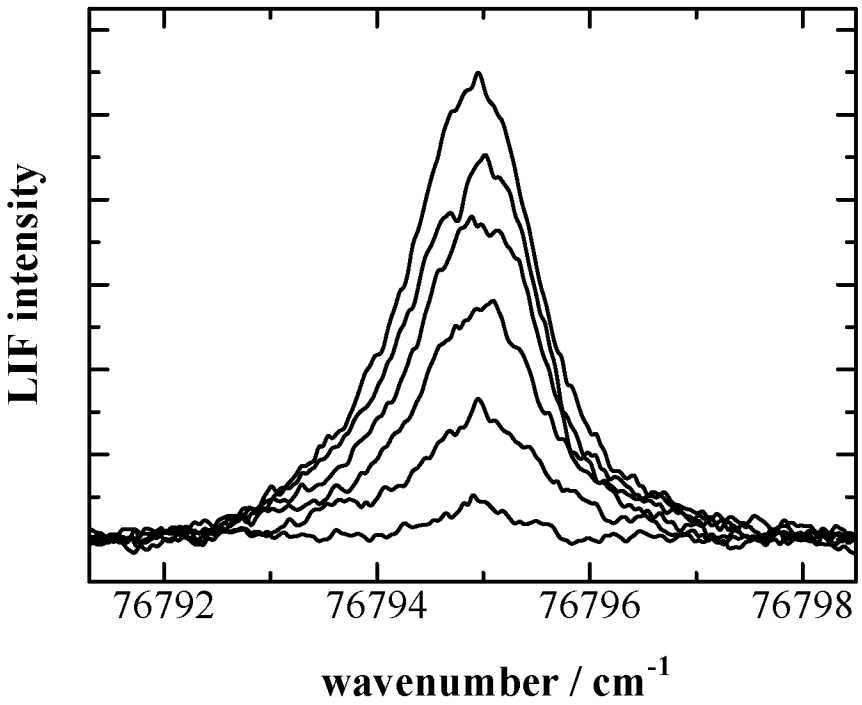


Fig. 4. H. Umemoto and M. Moridera

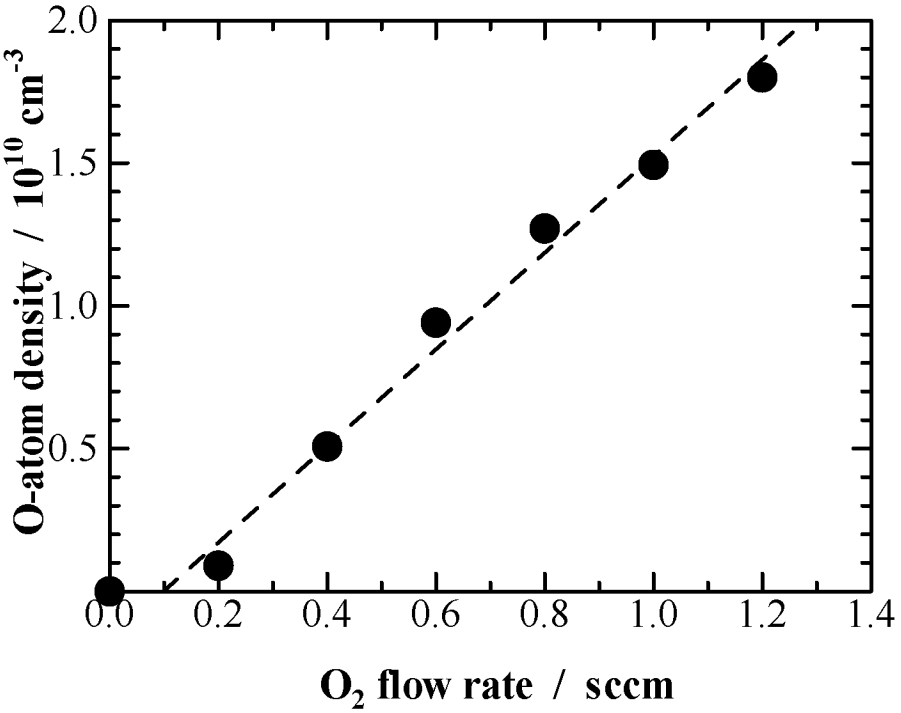


Fig. 5. H. Umemoto and M. Moridera

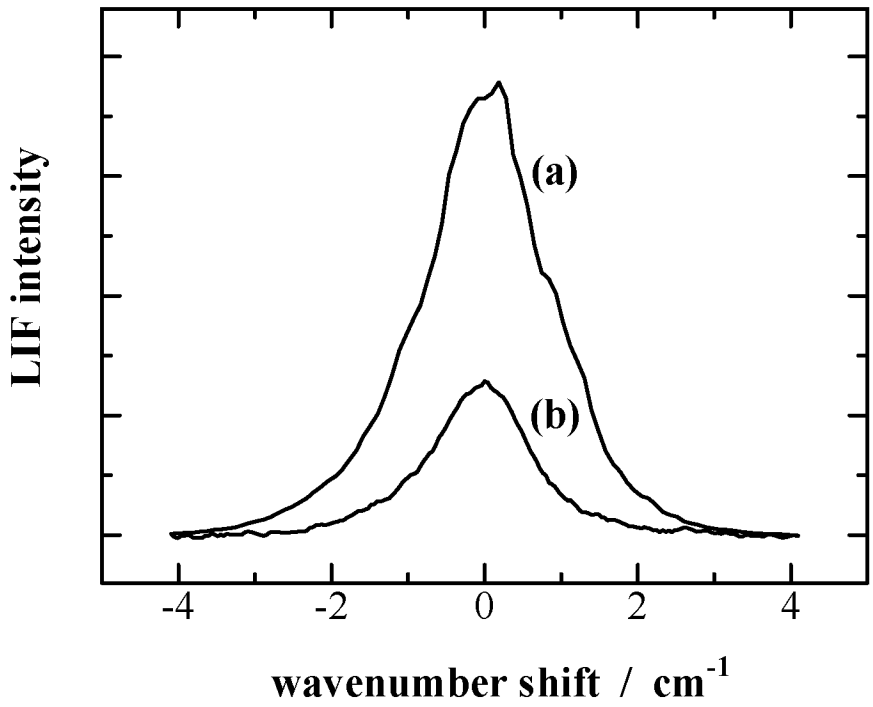


Fig. 6. H. Umemoto and M. Moridera

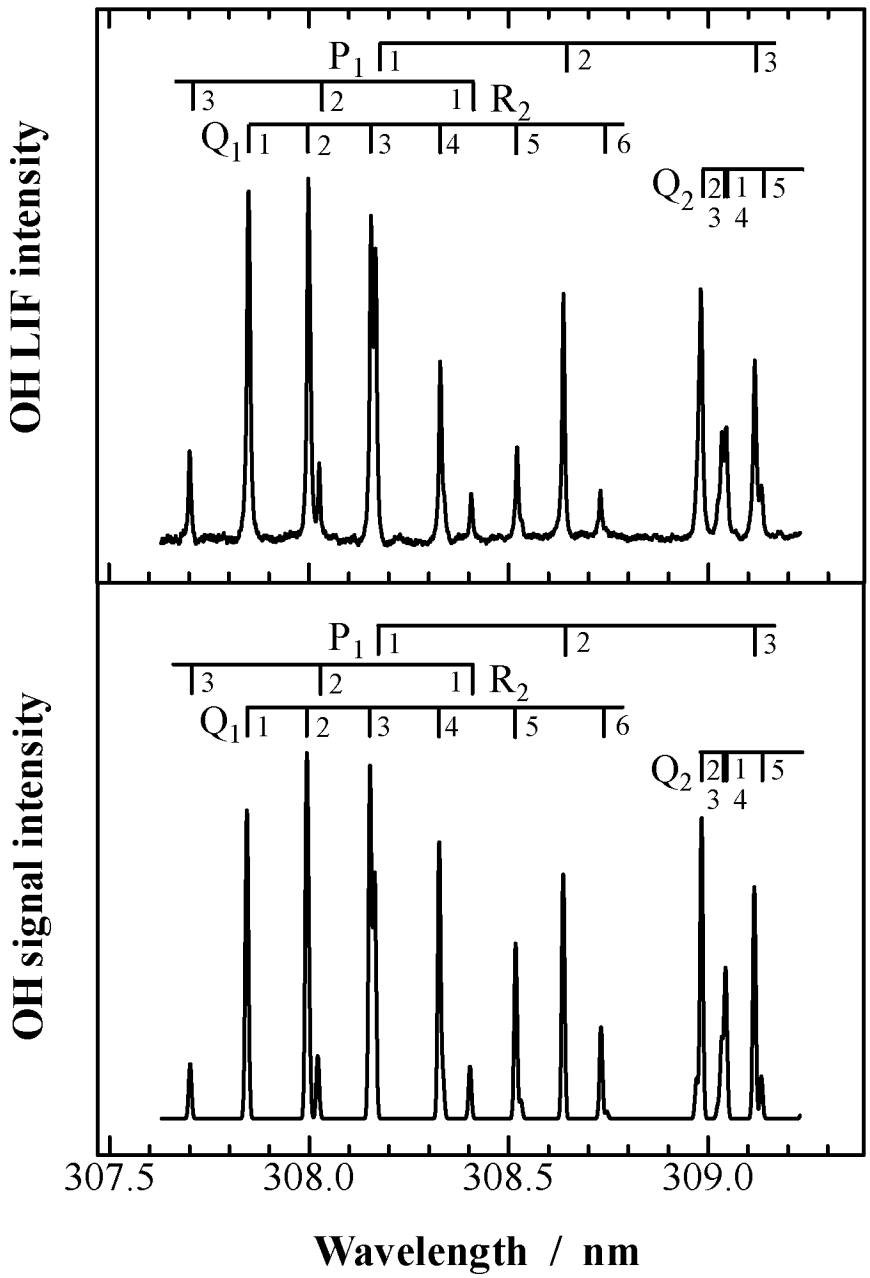


Fig. 7. H. Umemoto and M. Moridera

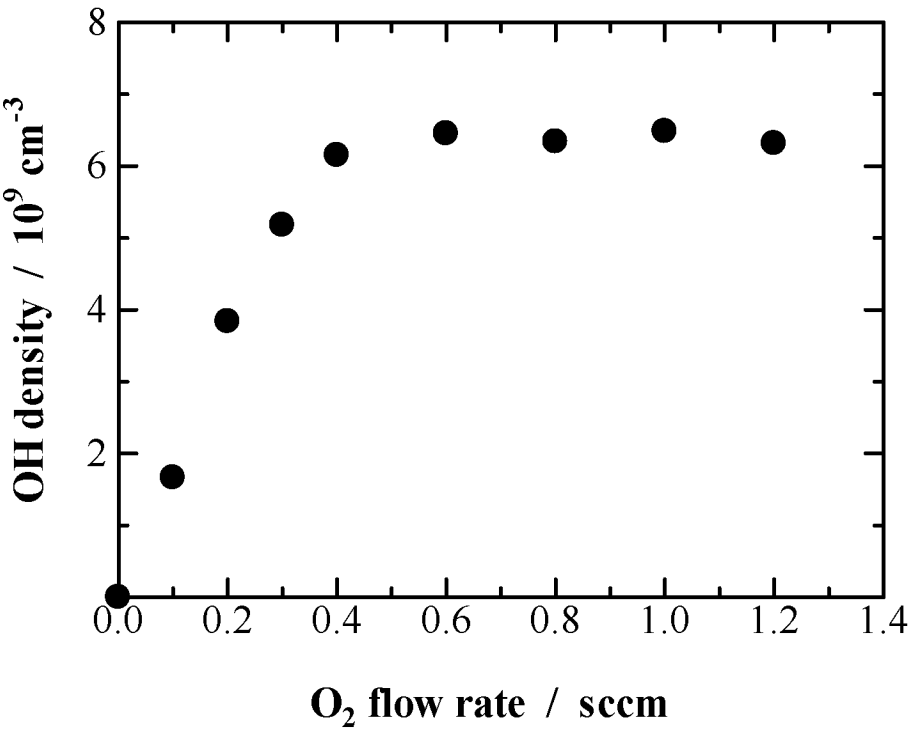


Fig. 8. H. Umemoto and M. Moridera

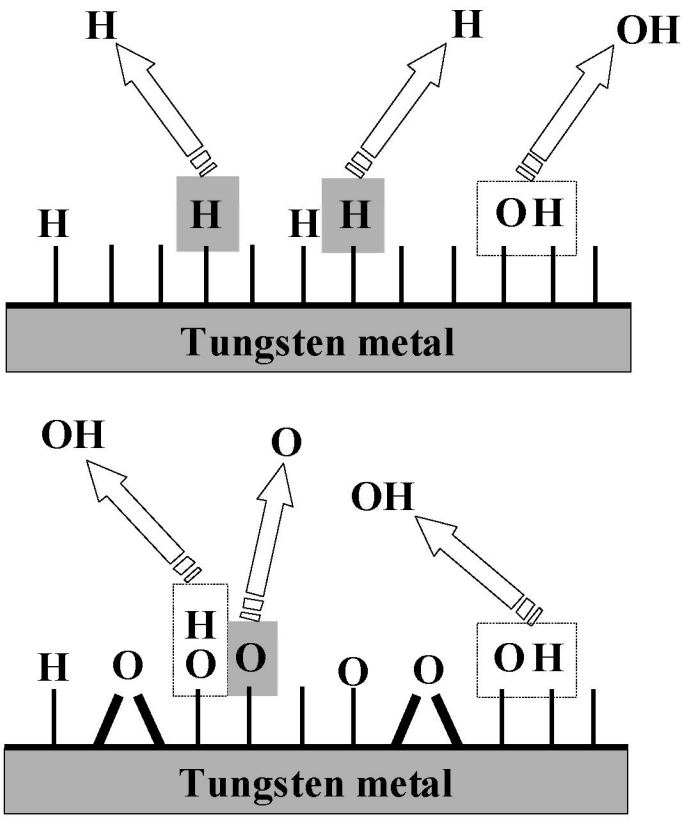


Fig. 9. H. Umemoto and M. Moridera